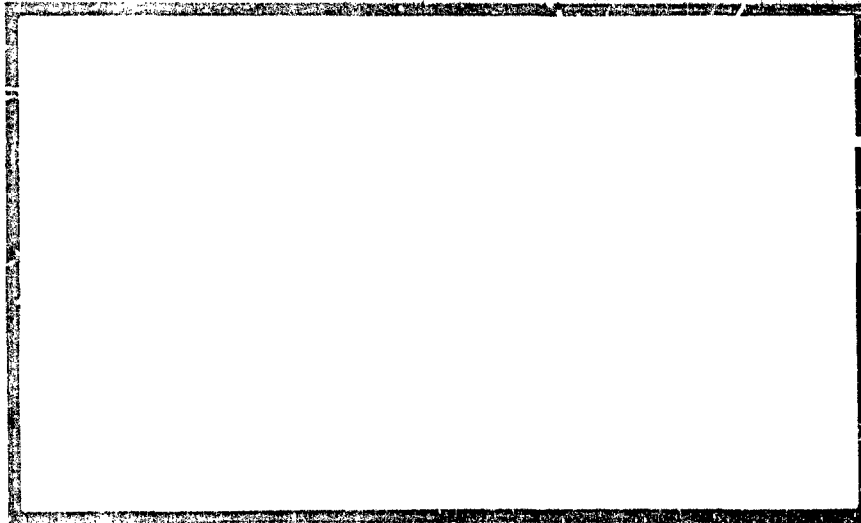


AD725026



Department of Mechanics and Hydraulics
COLLEGE OF ENGINEERING
THE UNIVERSITY OF IOWA

Iowa City, Iowa 52240

Approved for public release;
distribution unlimited.

D D C
RECEIVED
JUN 22 1971
REGULATED
B.

Reproduced by
NATIONAL TECHNICAL
INFORMATION SERVICE
Springfield, VA 22151

~~AIR MAIL~~

DOCUMENT CONTROL DATA - R & D

(Security classification of title, body of abstract and indexing annotation must be entered when the overall report is classified)

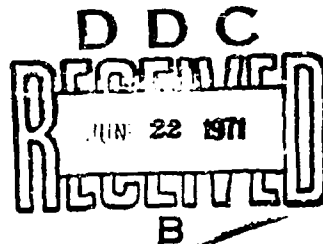
| | | | |
|---|---|--|--|
| 1. ORIGINATING ACTIVITY (Corporate author) | | 2a. REPORT SECURITY CLASSIFICATION | |
| University of Iowa Dept of Mechanics Iowa City, Iowa | | UNCLASSIFIED | |
| 2b. GROUP | | | |
| 3. REPORT TITLE | | | |
| A THEORY OF VISCOPLASTICITY WITHOUT A YIELD SURFACE PART II - APPLICATION TO MECHANICAL BEHAVIOR OF METALS | | | |
| 4. DESCRIPTIVE NOTES (Type of report and inclusive dates) | | | |
| Scientific Interim | | | |
| 5. AUTHOR(S) (First name, middle initial, last name) | | | |
| K. C. Valanis | | | |
| 6. REPORT DATE | 7a. TOTAL NO. OF PAGES | 7b. NO. OF REFS | |
| January 1971 | 32 | 5 | |
| 8a. CONTRACT OR GRANT NO. | 9a. ORIGINATOR'S REPORT NUMBER(S) | | |
| AFOSR 70-1916 | | | |
| b. PROJECT NO. | 9b. OTHER REPORT NO(S) (Any other numbers that may be assigned this report) | | |
| 9749 | AFOSR 71-1766 | | |
| c. 61102F | | | |
| d. 681304 | | | |
| 10. DISTRIBUTION STATEMENT | | | |
| Approved for public release; distribution unlimited. | | | |
| 11. SUPPLEMENTARY NOTES | | 12. SPONSORING MILITARY ACTIVITY | |
| TECH, OTHER | | Air Force Office of Scientific Research (NR) 1400 Wilson Boulevard Arlington, Virginia 22209 | |
| 13. ABSTRACT | | | |
| <p>The endochronic theory of viscoplasticity developed previously by the author is used to give quantitative analytical predictions on the mechanical response of aluminum and copper under conditions of complex strain histories. One single constitutive equation describes with remarkable accuracy and ease of calculation diverse phenomena, such as cross-hardening, loading and unloading loops, cyclic hardening as well as behavior in tension in the presence of a shearing stress, which have been observed experimentally by four different authors.</p> | | | |

A THEORY OF VISCOPLASTICITY
WITHOUT A YIELD SURFACE
PART II - APPLICATION TO MECHANICAL
BEHAVIOR OF METALS

A. C. Valanis
Professor of Mechanics
University of Iowa
Iowa City,
Iowa

Research sponsored by the Air Force Office
of Scientific Research, Office of Aerospace
Research, United States Air Force
under AFOSR Grant No. 70 - 1916

January 1971.



ABSTRACT

The endochronic theory of viscoplasticity developed previously by the author is used to give quantitative analytical predictions on the mechanical response of aluminum and copper under conditions of complex strain histories. One single constitutive equation describes with remarkable accuracy and ease of calculation diverse phenomena, such as cross-hardening, loading and unloading loops, cyclic hardening as well as behavior in tension in the presence of a shearing stress, which have been observed experimentally by four different authors.

where β is a positive constant. Note that $\beta > 0$ because $b_2^a > 0$, as well as $\frac{dy_D}{d\zeta} > 0$, thus necessitating that $f(\zeta) > 0$, for all ζ . As a result of Eq.'s (2.7) and (2.8),

$$z = \frac{1}{\beta} \log(1 + \beta\zeta) \quad (2.9)$$

an expression which has been found to give excellent agreement in the cases of some significant experiments, as will be shown in subsequent Sections.

In the absence of experimental data, the question of the form of the "relaxation" functions $\lambda(z)$ and $\nu(z)$ is equally difficult.

There are two simplifying assumptions, however, which lead to a relation between $\lambda(z)$ and $\nu(z)$, so that one is left with the problem of finding the form of only one of these functions. One is that of an elastic hydrostatic response and the other is the assumption of constant Poisson's ratio.

Efficient use of the first assumption is made by writing Eq. (1.1) in terms of the hydrostatic and deviatoric components of σ_{ij} , in which case

$$\sigma_{kk} = 3 \int_0^z K(z-z') \frac{\partial \epsilon_{kk}}{\partial z'} dz' \quad (2.10)$$

$$s_{ij} = 2 \int_0^z \mu(z-z') \frac{\partial \epsilon_{ij}}{\partial z'} dz' \quad (2.11)$$

where $K(z)$ is the bulk modulus. Elastic hydrostatic response implies that $K(z) = K_H(z)$, in which case Eq. (2.10) becomes,

$$\sigma_{kk} = 3K_{kk} \quad (2.12)$$

The assumption of constant Poisson ratio leads to the conclusion that $\nu(z)$ and $K(z)$ differ by a multiplicative constant, and can both be written

in terms of a single function $G(z)$, such that

$$K(z) = K_0 G(z) \quad (2.13)$$

$$\nu(z) = \nu_0 G(z) \quad (2.14)$$

where $G(0) = 1$.

This assumption has the added advantage that, under condition of plane stress, or uniaxial strain, the strain in the unstressed direction is related to the strains in the stressed directions by a multiplicative constant. Thus the strain increments in the direction of zero stress may be easily eliminated from the expression for $d\epsilon$, so that the latter may be expressed solely in terms of the strain increments in the stressed directions.

3. Crosshardening in tension-torsion

It has been observed that in aluminum and copper as well as in other metals, prestraining in torsion, well into the plastic range, has a significant hardening effect on the stress strain curve in tension.

In this Section we shall analyze data by Mair and Pugh, who have investigated this effect on annealed copper. Their experiments were performed accurately and with care, on very thin circular cylinders which were twisted well into the plastic region, so that upon unloading there remained a permanent residual shear strain. The effect of initial shear prestrain on the tensile response was then obtained by loading the cylinders in tension.

The constitutive equations pertinent to the above situation are easily found to be:

$$\sigma = \int_0^z E(z-z') \frac{de}{dz'} dz' \quad (3.1)$$

$$\tau = 2 \int_0^z \nu(z-z') \frac{d\eta}{dz'} dz' \quad (3.2)$$

where σ and ϵ are the axial stress and strain, respectively, and τ and η are the respective shear stress and torsional shear strain; the moduli $E(z)$ and $\nu(z)$ are interrelated through the bulk modulus $K(z)$. Their relating is best expressed through their Laplace transforms:

$$\bar{E} = \frac{3\bar{\nu}}{1 + \frac{\bar{\nu}}{3\bar{K}}} \quad (3.3)$$

To deal with the effect of cross-hardening analytically, we have assumed a constant poisson ratio. As a result Eq. (3.3) reduces to the form:

$$E(z) = E_0 G(z) \quad (3.4)$$

where

$$E_0 = \frac{3\nu_0}{1 + \frac{\nu_0}{3K_0}} \quad (3.5)$$

Regarding the form of $G(z)$ we have taken the simplest possible view by assuming that

$$G(z) = e^{-\alpha z} \quad (3.6)$$

Despite these simplifications we have been able to obtain excellent agreement with experimental data that have hitherto lacked analytical representation.

Analysis

In the tension-torsion test the effect of constant poisson ratio is to

reduce $d\zeta^2$ to the form

$$d\zeta^2 = k_1 d\epsilon^2 + k_2 d\eta^2 \quad (3.7)$$

where k_1 and k_2 are material constants, not the same as those in Eq. (1.6).

During torsion ($\epsilon=0$),

$$\zeta = k_2 \eta \quad (3.8)$$

whereas during tension ($\eta=\eta_0$) and after pretension

$$\zeta = k_2 \eta_0 + k_1 \epsilon \quad (3.9)$$

where η_0 is the maximum shear prestrain.

Equation (3.1) may now be written in the form

$$\sigma = E_0 \int_{\zeta_0}^{\zeta} G[z(\zeta) - z(\zeta')] \frac{\partial \epsilon}{\partial \zeta'} d\zeta' \quad (3.10)$$

(where $\zeta_0 = k_2 \eta_0$) when allowance is made of the fact that $\epsilon = 0$ in the range $0 \leq \zeta \leq k_2 \eta_0$. Thus cross-hardening is taken fully into account by Eq. (3.10), through the shear prestrain parameter ζ_0 , which appears as a lower limit on the integral on the right hand side of Eq. (3.10). If, in particular, we assume that $G(\zeta)$ is given by Eq. (3.6) and use of this is made in Eq. (3.10) the latter becomes

$$\sigma = E_0 e^{-\alpha z(\zeta)} \int_{\zeta_0}^{\zeta} \alpha z(\zeta') \frac{\partial \epsilon}{\partial \zeta'} d\zeta' \quad (3.11)$$

The integral in the right hand side of Eq. (3.11) can be evaluated explicitly by using Eq. (2.9) and noting that during monotonically increasing extension $\frac{d\epsilon}{d\zeta'} = k_1$. Omitting the algebra,

$$\sigma = \frac{E_0(1+\beta\zeta)}{k_1\beta n} \left(1 - \left(\frac{1+\beta\zeta}{1+\beta\zeta_0} \right)^{-n} \right) \quad (3.12)$$

where

$$n = 1 + \frac{a}{\beta} \quad (3.13)$$

and

$$\zeta_0 \leq \zeta = \zeta_0 + k_1\epsilon \quad (3.14)$$

Equation (3.12) represents a family of stress strain waves in tension, in terms of the prestrain parameter ζ_0 and the "cross-hardening" parameter^a β .

To determine the material parameters in Eq. (3.12) we note that in the absence of shear prestrain ($\zeta_0 = 0$),

$$\sigma = \frac{E_0(1+\beta_1\epsilon)}{\beta_1 n} \left(1 - (1+\beta_1\epsilon)^{-1} \right) \quad (3.15)$$

where $\beta_1 = k_1\beta$.

It may be verified that as $\epsilon \rightarrow 0$, $\sigma = E_0\epsilon$ i.e. E_0 is the initial slope of the stress-strain curve. Also as ϵ increases, σ tends asymptotically to the linear expression

$$\sigma = \frac{E_0}{\beta_1 n} (1+\beta_1\epsilon) \quad (3.16)$$

* There is ample justification for calling β the cross-hardening parameter.

Indeed in the limit of $\beta = 0$, and using Eq. (3.9) Eq. (3.12) becomes:

$$\sigma = \frac{E_0}{k_1 a} (1 - e^{-a\epsilon})$$

which is independent of ζ_0 ; in other words cross-hardening cannot take place when $\beta = 0$, as pointed out earlier.

If E_t is the slope (tangent modulus) of the asymptotic straight line, then

$$n = \frac{E_o}{E_t} \quad (3.17)$$

Also, as shown in Fig. 1, if one extrapolates backwards the asymptotic straight line to intersect the stress axis one obtains an intercept σ_o from which β_1 is determined by the relation

$$\beta_1 = \frac{E_t}{\sigma_o} \quad (3.18)$$

Similarly integration of Eq. (3.2) yields an equation analogous to Eq. (3.16); this is

$$\tau = \frac{2u_o(1+\beta_2 n)}{\beta_2 n} \{1 - (1+\beta_2 n)^{-n}\} \quad (3.19)$$

where $\beta_2 = k_2 \beta$. Thus, β_2 and u_o may be determined from Eq. (3.19).

Finally we observe from Eq. (3.12) that the intercepts σ_o' in the presence of shear prestrain ζ_o are given from the expression

$$\sigma_o' = \sigma_o (1+\beta \zeta_o) = \sigma_o (1+\beta_2 n_o) \quad (3.20)$$

Equation (3.20) was used to confirm the self-consistency of the theory. However Eq.'s (3.12), (3.1) and (3.19) can only yield the ratio $\left(\frac{k_1}{k_2}\right)$ but the constants k_1 and k_2 cannot be evaluated. In this sense, and for these experiments one may choose k_2 arbitrarily; we chose $k_2 = 1$.

Experimental data obtained by Mair and Pugh that illustrate the effect of cross-hardening are given in Fig. 2.

Curve 0 is the virgin stress strain curve for the type of copper they used. The circles on the curves A, B and C are experimental points corres-

ponding to initial shear prestrains of $.25 \times 10^{-2}$, 1.5×10^{-2} and 3×10^{-2} respectively.

From curve 0, $E_0 = 14 \times 10^6$ lb/in², $\beta_1 = .53 \times 10^2$, $n = 46$. With $k_2 = 1$, Eq. (3.20) was used to give $k = 1.00$. The curves A, B and C were then calculated and plotted as shown. Without a doubt the agreement between theory and experiment is remarkable.

4. Repetitive loading-unloading cycles

The tensile strain history $\epsilon(\zeta)$ corresponding to a typical tensile loading-unloading sequence is shown in Fig. 3. We use the terms "straining" and "unstraining" in the following sense:

The ranges $0 \leq \zeta < \zeta_1$, $\zeta_2 \leq \zeta < \zeta_3$, $\zeta_B \leq \zeta < \zeta_5$, $\zeta_D \leq \zeta$ represent straining in tension.

The ranges $\zeta_1 \leq \zeta < \zeta_2$, $\zeta_3 \leq \zeta < \zeta_A$, $\zeta_5 \leq \zeta < \zeta_C$ represents unstraining in tension.

The ranges $\zeta_A \leq \zeta < \zeta_4$, $\zeta_6 \leq \zeta < \zeta_8$, $\zeta_7 \leq \zeta < \zeta_8$ represent straining in compression.

The ranges $\zeta_4 \leq \zeta < \zeta_B$, $\zeta_6 \leq \zeta < \zeta_7$, $\zeta_8 \leq \zeta < \zeta_D$ represent unstraining in compression.

Points on the ζ -axis denoted by ζ_r ($r=1,2,\dots$) represent points of discontinuity in $\frac{d\epsilon}{d\zeta}$, brought about by reverting from straining to unstraining histories, or vice-versa.

A perusal of experimental data on copper, shows that the constitutive equation of the metal varies depending on its previous history of manufacture and subsequent annealing. The single term form of $G(\zeta)$ that explained Mair and Pugh's data⁽²⁾ so well was found inadequate to explain data by Lubahn⁽³⁾

and by Wadsworth⁽⁴⁾,

We found, however, that the adoption of a single extra term for $G(z)$ suffices to describe quantitatively broad trends of their data. In effect we took

$$G(z) = E_1 + G_2 e^{-az} \quad (4.1)$$

or

$$E(z) = E_1 + E_2 e^{-az} \quad (4.2)$$

Let ζ_n ($n = 1, 2, \dots$) be the last point of discontinuity in $\frac{d\epsilon}{d\zeta}$. Then using Eq's. (2.9), (3.11) and (4.1) and in the range $\zeta_m \leq \zeta$

$$\sigma = (1+\beta\zeta)\sigma_0 \left\{ (-1)^m - \frac{1}{(1+\beta\zeta)^n} + 2 \sum_{r=1}^m (-1)^{r+1} \frac{(1+\beta\zeta_r)^n}{1+\beta\zeta} \right\} + E_1 \epsilon \quad (4.3)$$

The quantities ζ_r may be evaluated explicitly in terms of ϵ_r (the values of strain corresponding to ζ_r) by the formula

$$\zeta_r = 2k_1 \sum_{s=1}^r (-1)^{s-1} \epsilon_s + k_1 (-1)^r \epsilon_r \quad (4.4)$$

The effect of E_1 on the unstraining characteristics is remarkable, especially since its effect on the shape of the straining part of the stress-strain curve is minimal. Let the history $\epsilon(z)$ be one of continuous straining. Then Eq. (4.3) becomes:

$$\sigma = E_1 \epsilon + \frac{E_2 (1+\beta_1 \epsilon)}{n\beta_1} (1 - (1+\beta_1 \epsilon)^{-n}) \quad (4.5)$$

From Eq. (4.5) we obtain the following relations in the notation of Section 3.

$$E_1 + E_2 = E_0 \quad (4.6a)$$

$$\frac{2}{\beta_1^n} = \sigma_0 \quad (4.6b)$$

$$E_1 + \sigma_0 \beta_1 = E_t \quad (4.6c)$$

Equations (4.6a-c) do not suffice for the determination of the four unknown material constants E_1 , E_2 , n , β_1 . It has been found that a fourth relation can be obtained by considering the "unloading" portion of the stress-strain history.

Fig. 4, shows the stress-strain relation for a uniaxial specimen which has been strained in tension to a strain value ϵ_1 , whereupon it is unloaded and compressed until the final strain is zero.

The strain-intrinsic time measure history $\epsilon(\zeta)$ corresponding to the above stress-strain history is also shown in Fig. 5.

Equation (4.3) in conjunction with the above history yields the relation, at $\epsilon = 0$:

$$\sigma = \sigma_0 (1 + \beta \zeta) \left\{ -1 + \frac{2(1 + \beta \zeta_1)^n - 1}{(1 + \beta \zeta)^n} \right\} \quad (4.7)$$

If the value of ϵ_1 is sufficiently large (in the case of copper this value was found to be 50×10^{-3} , or so) then σ_0^c is given very nearly by the expression

$$\sigma_0^c = -\sigma_0 (1 + 2\beta \zeta_1) = -\sigma_0 (1 + 2\beta_1 \epsilon_1) \quad (4.8)$$

The constant β_1 can now be obtained from Eq. (4.8) and the constants E_1 , E_2 and n can be found from Eq's. (4.6a-c).

We illustrate the points made in the above discussion in Fig. 6 where stress

strain curves for three different materials are given when these are subjected to the same strain history shown in Fig. 5.

The constants for these materials are given in the following table:

| | E_1 | E_2 | B | n |
|---|-------------------|--------------------|------------------|-----|
| 1 | 0 | 6.14×10^6 | $.4 \times 10^2$ | 25 |
| 2 | $.24 \times 10^6$ | 5.9×10^6 | 0 | - |
| 3 | $.12 \times 10^6$ | 6.02×10^6 | $.2 \times 10^2$ | 50 |

What is remarkable is that changing B results in these materials having indistinguishable stress-strain curves during straining but wildly differing ones during unstraining.

In Fig. 7 we illustrate an attempt to predict analytically the loading-unloading-loading response of copper in simple tension. The solid line is an experimental curve obtained by Lubahn⁽³⁾ for a copper specimen which had already undergone similar strain cycles. We have assumed, however, that these have a negligible effect in the response shown because they occurred sufficiently far in the distant "past".

The triangular points shown, were obtained theoretically from Eq. (4.3) by assuming that the specimen was continually extended (without unstraining) until the strain $\epsilon = 51.6 \times 10^{-3}$ was reached. The unstraining-straining cycle was then applied.

Despite the fact that $E(z)$ was approximated by two terms, as in Eq. (4.2) the agreement between theory and experiment is remarkable. The constants employed were, $\sigma_0 = 6 \times 10^3$, $E_1 = .125 \times 10^6$, $B = .02 \times 10^3$, $n = 160$.

In fact we are not aware of another instance where an attempt was made to describe such experimental data analytically by means of one single

constitutive equation. In addition we can say with assurance that the observed difference between theory and observation can be reduced further by including more exponential terms in the series representation for $E(z)$. We conclude this Section by considering the effect of work hardening under cyclic straining. In particular we shall examine the work of Wadsworth's⁽⁴⁾ and show that our theory again provides an excellent analytical basis for his results.

In this work single copper crystals were tested under conditions of uniaxial cyclic strain; The data was presented in terms of the resolved shear stress and strain in the plane of slip.

Fig. 8 gives the first few cycles of his straining program, in which a crystal was cycled under fixed limits of resolved shear strain of 7×10^{-3} . The "peak stresses" corresponding to the extreme values of tensile and compressive strain increased monotonically with the number of cycles.

In Fig. 9 the values of peak tensile and compressive stresses have been plotted by Wadsworth against $|d\eta|$. It is rather interesting that he felt that such a plot was meaningful, without further elaboration on this point. Of course $|d\eta|$, but for a scalar factor, is our intrinsic time measure.

The history of the resolved shear strain versus ξ is shown in Fig. 10. From this Figure it follows that $\xi_m = (2m-1)\Delta k_1$. Equations (4.6c) and (4.8) were now utilized to find βk_1 , which we denote by β_1 , and E_1 . It was found that $\beta_1 = 12.3$ and $E_1 = 2 \times 10^9 \frac{\text{dyn}}{\text{cm}^2}$. At this point n could not be determined because the initial slope of the stress-strain curve corresponding to ξ_1 could not be evaluated accurately.

However letting $\tau_m \equiv \tau|_{\xi=\xi_m}$, it was found that as $m \rightarrow \infty$, Eq. (4.3)

yields the asymptotic expression:

$$\tau = nB\tau_0 \Delta + E_1 \Delta \quad (4.9)$$

Hence, from the tensile experimental curve of Fig. 4 of Ref. 4, n could be determined explicitly and was found to be equal to 225. For this value of n the term $\frac{1}{(1+B\tau_m)} n$ was found to be negligible for $m \geq 1$.

Thus for the history in Fig. 10, Eq. (4.3) gives

$$\tau_{m+1} = \tau_0 [1+B_1(2m+1)\Delta] (-1)^{m+2} \prod_{r=1}^m \left[\frac{1+(2r-1)B_1\Delta}{1+(2m+1)B_1\Delta} \right]^n (-1)^{r+1} + E_1 r \quad (4.10)$$

The above equation can be simplified further for large values of m . In particular for $m \geq 50$, it was found that the series in the bracket on the right hand side of Eq. (4.10) degenerates into the geometric series

$$\prod_{r=1}^m (-u)^r \sim -\frac{u}{1+u} \quad (4.11)$$

where

$$u = \left\{ \frac{1+(2m-1)B_1\Delta}{1+(2m+1)B_1\Delta} \right\}^n \quad (4.12)$$

Equation (4.10) may now be written in an asymptotic form in terms of the absolute value of the shear stress as follows:

$$|\tau_m| = (1+B(2m+1)\Delta) \tau_0 \left(-1 + \frac{2}{1+u} \right) + E_1 \Delta \quad (4.13)$$

For very large values of m ($m \gg n$) Eq. (4.13) simplifies further and becomes

$$|\tau_m| = \frac{nB_1\tau_0\Delta}{1-\frac{n}{m}} + E_1\Delta \quad (4.14)$$

Thus,

$$\lim_{m \rightarrow \infty} |\tau_m| = n\beta_1 \tau_0 \Delta + E_1 \Delta \quad (4.15)$$

In Fig. 11 a plot has been made of the theoretical relation between $|\tau_m|$ and $m\Delta$ obtained from Eq. (4.13). The experimental points obtained by Wadsworth are also shown. The following comments are in order. Though our theory does give values for τ_m which are different in tension from those in compression, the difference is not as great as the experimental data indicate, and is too small to be plotted on the scale shown. However, the theoretical curve lies very close to, and is in fact bounded by the experimental points, which indicate a deviation between the values of compressive stress and those of tensile stress which increases with m but is never greater than 5.5%.

This is the first time that a theory of plasticity has provided a rational explanation for the phenomena of cyclic hardening.

5. Tensile response in the presence of initial shear stress

In Section 3 we obtained a theoretical prediction of the effect of prestrain in torsion on the stress strain curve in tension. In this Section we shall examine theoretically, in the light of our endochronic theory, the effect of initial constant prestress in torsion on the stress-strain curve in tension. To do this, we have assumed, just as we did in Section 3, that $E(z)$ and $\nu(z)$ are proportional to some relaxation function $G(z)$, and furthermore that $G(z)$ consists of a single exponential term i.e. it is given by Eq. (3.6). Thus

$$E(z) = E_0 e^{-\alpha z} \quad (5.1)$$

In the light of Eq. (5.1) and bearing in mind Eq. (2.9), the constitutive Eqs (3.1) and (3.2) can be reduced to the differential equations

$$E_0 \frac{d\epsilon}{d\zeta} = \frac{\alpha\sigma}{1+\beta\zeta} + \frac{d\sigma}{d\zeta} \quad (5.2)$$

$$2\mu_0 \frac{d\eta}{d\zeta} = \frac{\alpha\tau}{1+\beta\zeta} + \frac{d\tau}{d\zeta} \quad (5.3)$$

where, as in Section 3,

$$d\zeta^2 = k_1 d\epsilon^2 + k_2 d\eta^2 \quad (5.4)$$

As mentioned above the test to be discussed consists of applying an initial stress τ^0 corresponding to an initial strain η_0 ; then keeping τ^0 constant, a axial strain ϵ is applied and the axial stress σ is measured. The object at hand is to deduce from Eq.'s (5.1-5.4) the relation between σ and ϵ , and compare with the experimental data obtained by Ivey⁽⁵⁾.

To accomplish this we proceed as follows. From Eq. (5.4) it is clear that the axial straining process begins at $\zeta = \zeta_0$ where

$$\zeta_0 = k_2 \eta_0 \quad (5.5)$$

During this process $\frac{d\tau}{d\zeta} = 0$, so that from Eq. (5.3)

$$d\eta = \frac{\alpha\tau^0}{2\mu_0} \frac{d\zeta}{1+\beta\zeta} \quad (5.6)$$

Equations (5.4) and (5.6) now combine to show that during the axial straining process,

$$d\zeta^2 = k_1^2 d\epsilon^2 + k_2^2 \left(\frac{\alpha\tau^0}{2\mu_0} \right)^2 \frac{d\zeta^2}{(1+\beta\zeta)^2} \quad (5.7)$$

At this point we introduce the variable θ such that

$$\zeta = k_1 \theta \quad (5.8)$$

Also let $(\frac{k_2}{k_1}) = k$, $k_1 B = \beta$ and $c = (k\alpha^0/2\mu_0)$. Then, in terms of θ and as a result of Eq. (5.7)

$$d\theta \left\{ 1 - \frac{c^2}{(1+\beta_1 \theta)^2} \right\}^{\frac{1}{2}} = d\epsilon \quad (5.8)$$

Equation (5.8) may be integrated subject to the initial condition that at $\zeta = k_2 \eta_0$, $\epsilon = 0$; or, $\theta = \theta_0 = k\eta_0$, $\epsilon = 0$.

Equation (5.2) may now be integrated with respect to θ to yield

$$\sigma = \frac{E_0}{(1+\beta_1 \theta)(\alpha/\beta_1)} \int_{\theta_0}^{\theta} (1+\beta_1 \theta')^{(\alpha/\beta_1 - 1)} \sqrt{(1+\beta_1 \theta')^2 - c^2} d\theta' \quad (5.9)$$

We introduce now a change of variable by the relation

$$1 + \beta_1 \theta = c \cosh \phi \quad (5.10)$$

whereupon Eq. (5.9) becomes:

$$\sigma = \frac{E_0 c}{\beta_1 \cosh^{n-1} \phi} \int_{\phi_0}^{\phi} (\cosh^n \phi' - \cosh^{n-2} \phi') d\phi' \quad (5.11)$$

where as before, $n = 1 + \frac{\alpha}{\beta_1}$.

Now,

$$\int \cosh^n x dx = \frac{n-1}{n} \int \cosh^{n-2} x dx + \frac{1}{n} \cosh^{n-1} x \sinh x \quad (5.12)$$

Since for asymptotically large n (say $n \geq 30$), $\frac{n-1}{n} \sim 1$, it follows from Eq. (5.12) that in this instance

$$(\cosh^n x - \cosh^{n-2} x) dx \sim \frac{1}{n} \cosh^{n-1} x \sinh x \quad (5.13)$$

The result of Eq. (5.13) can be utilized to obtain a closed form solution for σ which now becomes,

$$\sigma = \frac{E_0 c}{\beta_1 n} \left\{ \sinh\phi - \left(\frac{\cosh\phi_0}{\cosh\phi} \right)^{n-1} \sinh\phi_0 \right\}. \quad (5.14)$$

Equation (5.8) may also be integrated with respect to ϕ to yield

$$\epsilon = \frac{c}{\beta_1} \{ F(\phi) - F(\phi_0) \} \quad (5.15)$$

where

$$F(\phi) \equiv \sinh\phi - \tan^{-1}(\sinh\phi) \quad (5.16)$$

Thus σ and ϵ are related parametrically through ϕ and ϕ_0 such that

$$\phi_0 = \cosh^{-1} \left(\frac{(1 + \beta_1 k \eta_0)}{c} \right) \quad (5.17)$$

The relation between σ and ϵ has been calculated with the following values of the constants:

$$k = 1, \sigma_0 = \frac{E_0}{\beta_1 n} = 17.4 \times 10^3 \text{ lb/in}^2, \beta = 20, n = 33.$$

The result was compared with one of Ivey's experiments in which $\tau^0 = 14 \times 10^3 \text{ lb/m}^2$, $\eta_0 = 2.35 \times 10^{-3}$. The predicted and experimental stress-strain responses compare very favorably. See Fig. 12.

Conclusion

On the evidence of the results presented above it appears that the endochronic theory of plasticity can predict accurately the mechanical response of metals under complex straining histories. The full implications of the theory will be investigated further in our future work.

References

1. Valanis, K. C., "A Theory of Viscoplasticity without a yield surface, Part I - General Theory", Mechanics Report 1.01, University of Iowa, Dec. 1970.
2. Mair, W. M. and Pugh, H. L. D., "Effect of Prestrain on Yield Surfaces in Copper", J. Mech. Eng. Sc., 6, 150, (1964).
3. Lubahn, J. D., "Bauschinger Effect in Creep and Tensile Tests on Copper", J. of Metals, 205, 1031, (1955).
4. Wadsworth, M. J., "Work Hardening of Copper Crystals under Cyclic Straining", Acta Metallurgica, 11, 663, (1963).
5. Ivey, H. J. "Plastic Stress Strain Relations and Yield Surfaces for Aluminum Alloys", J. Mech. Eng. Sc., 3, 15, (1961).

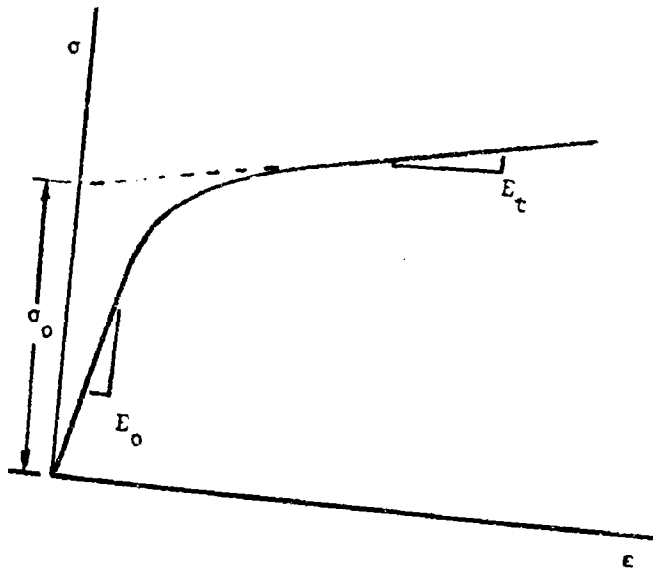


Fig. 1. Typical stress-strain curve

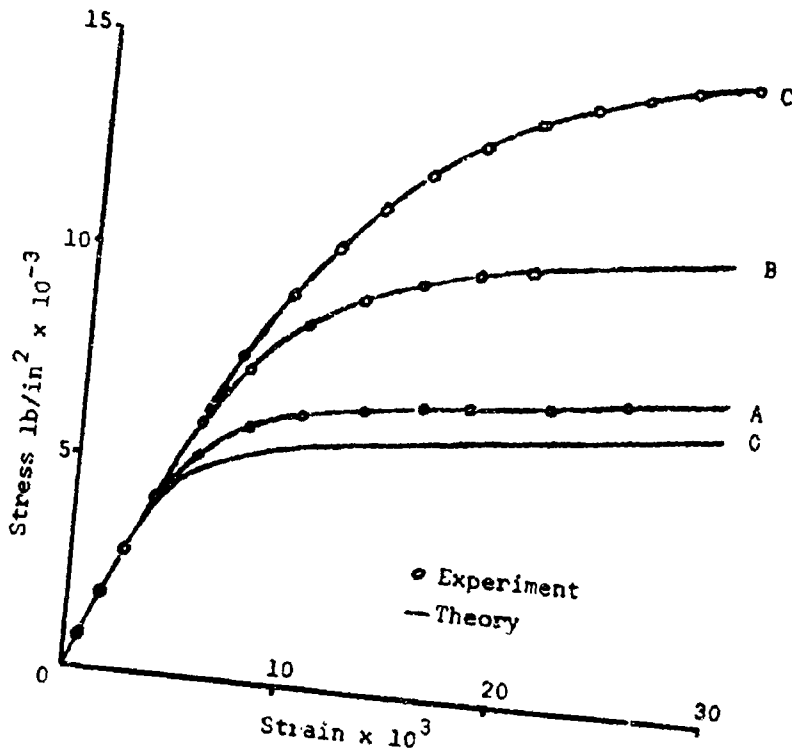


Fig. 2. Hardening due to shear prestrain

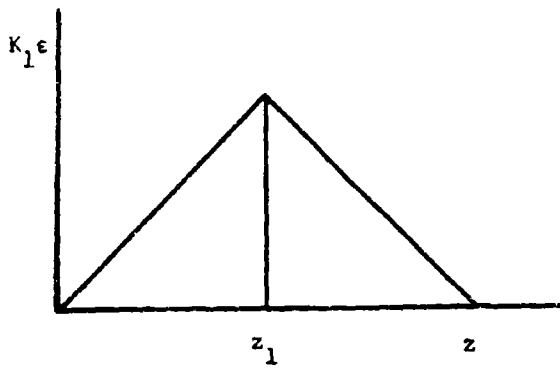


Fig. 5. Strain history of Fig. 6.

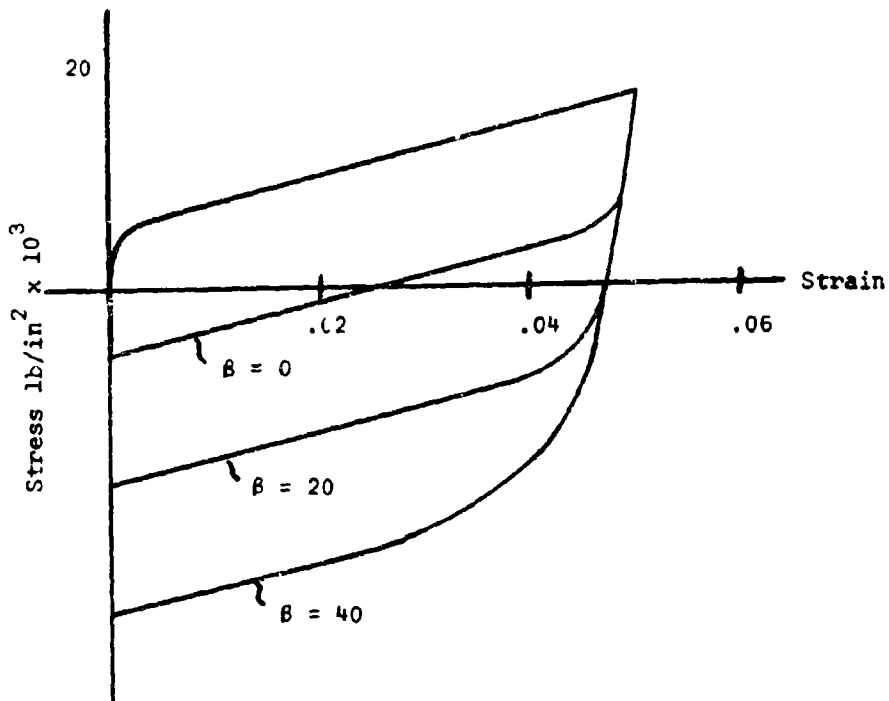


Fig. 6. Bauschinger effect and its relation to B

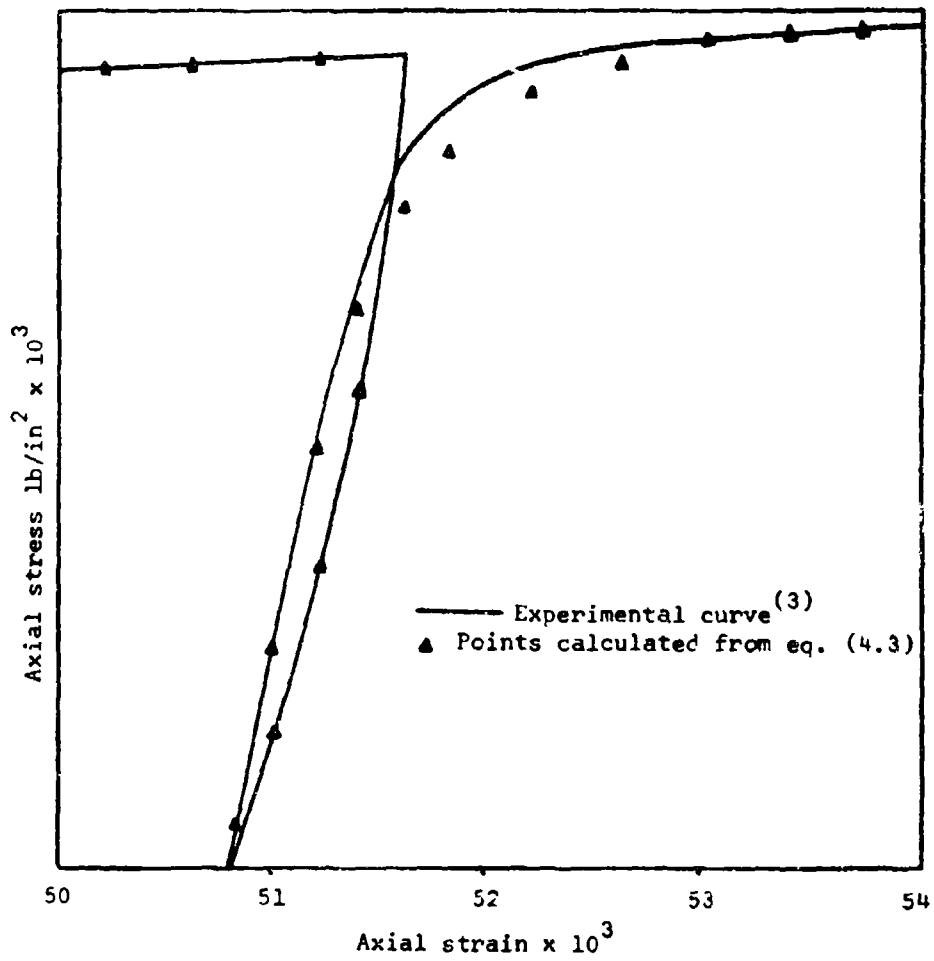


Fig. 7. Unloading - loading loop

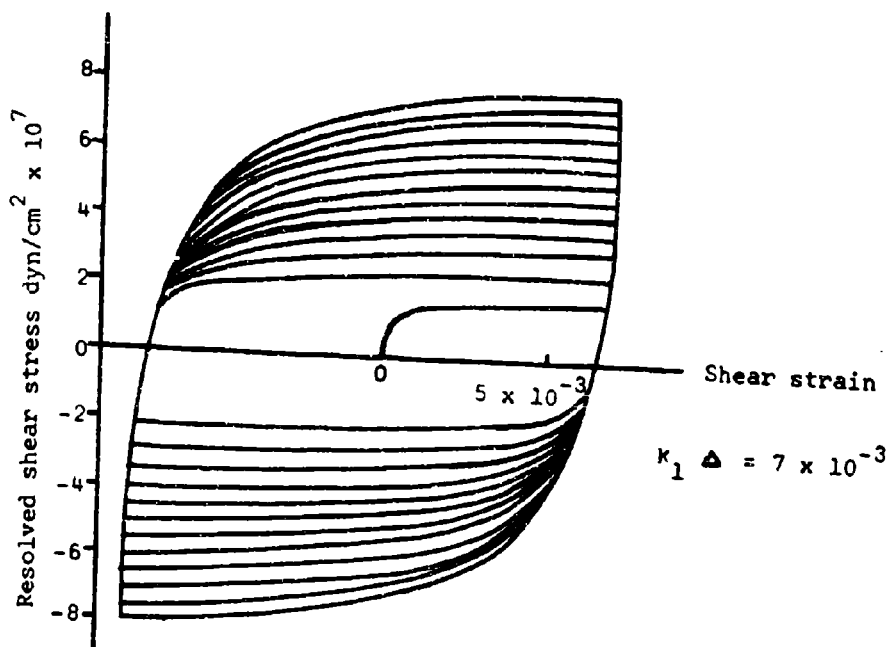
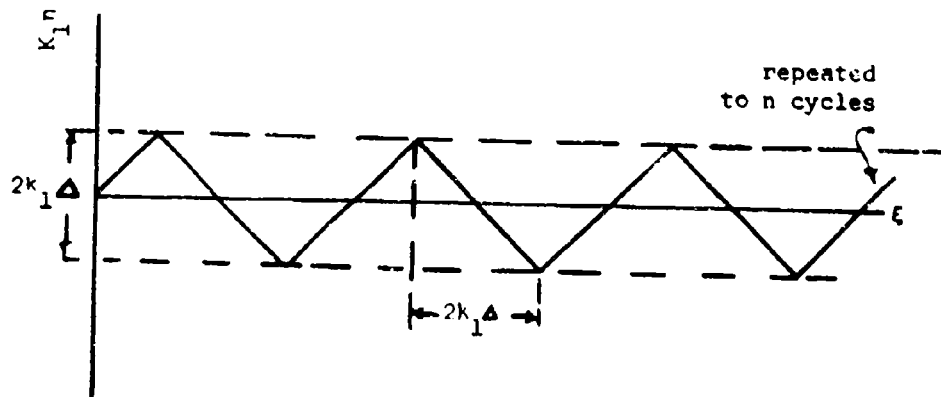


Fig. 8. Cyclic straining

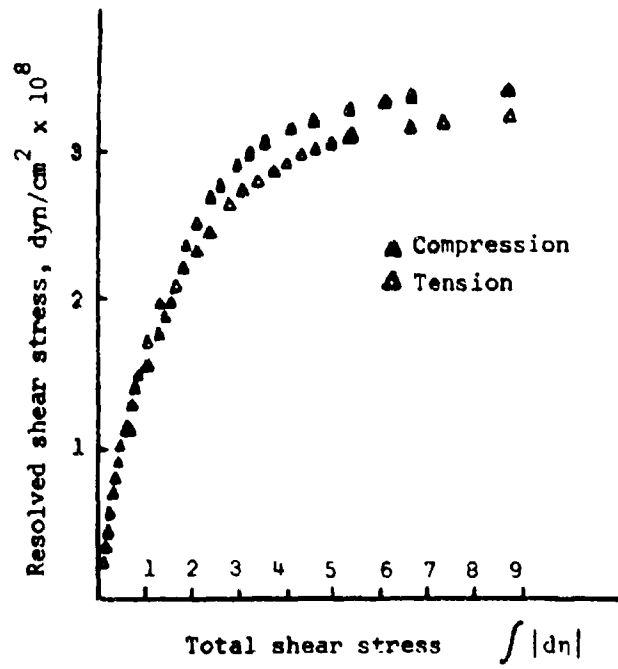


Fig. 9. Peak stresses due to cyclic straining

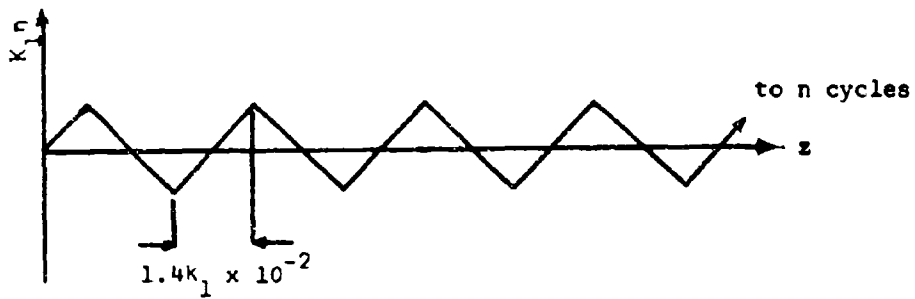


Fig. 10. History of resolved shear strain

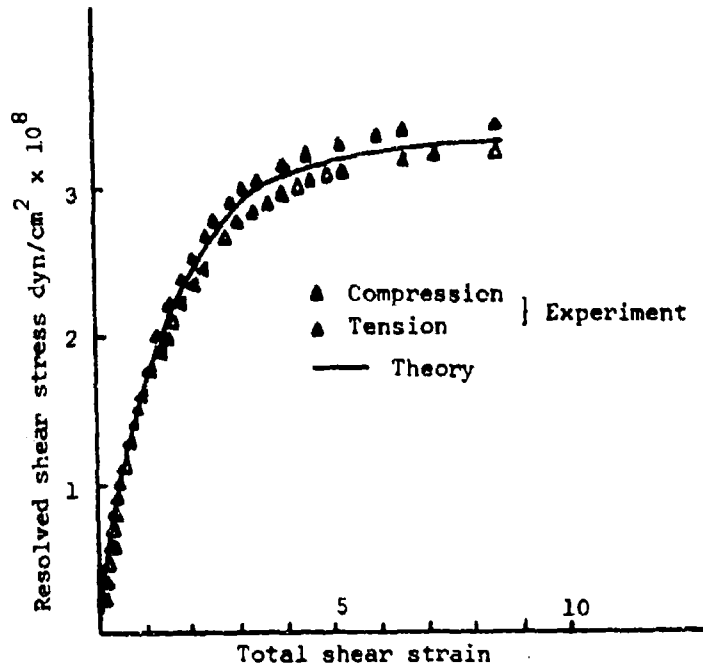


Fig. 11. Theoretical prediction of cyclic hardening

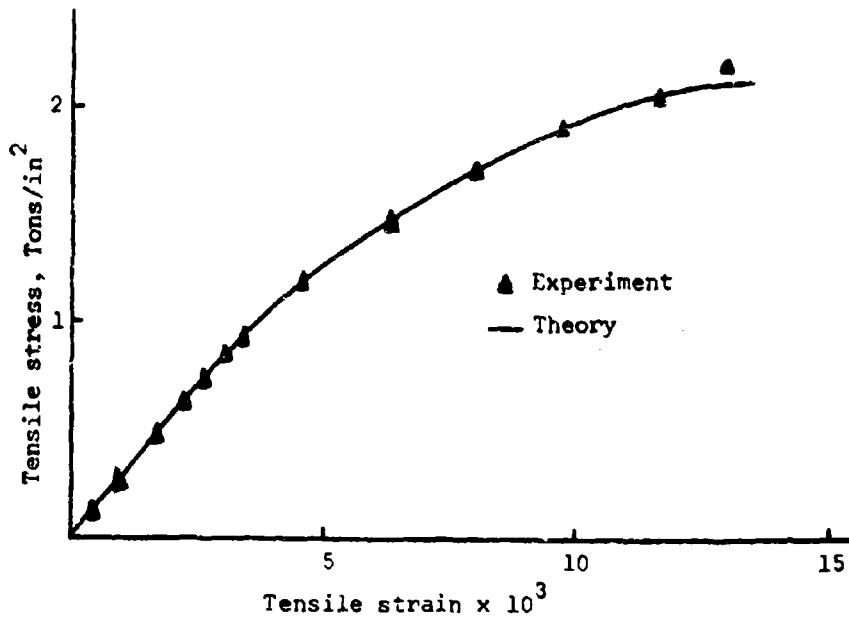


Fig. 12. Theoretical prediction of effect of shear prestress